Prostate-Speci#c Membrane Antigen Targeted Therapy of Prostate Cancer Using a DUPA–Paclitaxel Conjugate

Qingzhi Lv, Jincheng Yang, Ruoshi Zhang, Zimeng Yang, Zhengtao Yang, Yongjun Wang, Youjun Xu, and Zhonggui He

Mol. Pharmaceutics, **Just Accepted Manuscript** • DOI: 10.1021/acs.molpharmaceut.8b00026 • Publication Date (Web): 02 Apr 2018

Prostate-Specific Membrane Antigen Targeted Therapy of Prostate Cancer Using a DUPA–Paclitaxel Conjugate

Qingzhi Lv,[†‡] Jincheng Yang,[§] Ruoshi Zhang,[†] Zimeng Yang,[†] Zhengtao Yang,[§] Yongjun Wang,[†] Youjun Xu,*[§] Zhonggui He*[†]*

[†]Wuya College of Innovation, Shenyang Pharmaceutical University, 103 Wenhua Road, Shenyang, 110016, China

[‡]School of Pharmacy, Binzhou Medical University, 346 Guanhai Road, Yantai 264003, China

[§]Key Laboratory of Structure-Based Drug Design & Discovery of Ministry of Education, Shenyang Pharmaceutical University, 103 Wenhua Road, Shenyang 110016, China

Key words: Paclitaxel; Prostate-specific membrane antigen; DUPA; Prostate cancer; Disulfide bond

ABSTRACT

Prostate cancer (PCa) is the most prevalent cancer among men in the United States and remains the second-leading cause of cancer mortality in men. Paclitaxel (PTX) is

the first line chemotherapy for PCa treatment, but its therapeutic efficacy is greatly restricted by the non-specific distribution *in vivo*. Prostate-specific membrane antigen (PSMA) is overexpressed on the surface of most PCa cells and its expression level increases with cancer aggressiveness, while being present at low levels in normal cells. The high expression level of PSMA in PCa cells offers an opportunity for target delivery of nonspecific cytotoxic drugs to PCa cells, thus improving therapeutic efficacy and reducing toxicity. PSMA has high affinity for DUPA, a glutamate urea ligand. Herein, a novel DUPA−PTX conjugate is developed using DUPA as the targeting ligand to deliver PTX specifically for treatment of PSMA expressing PCa. The targeting ligand DUPA enhances the transport capability and selectivity of PTX to tumor cells via PSMA mediated endocytosis. Besides, DUPA is conjugated with PTX via a disulfide bond, which facilitates the rapid and differential drug release in tumor cells. The DUPA−PTX conjugate exhibits potent cytotoxicity in PSMA expressing cell lines and induces a complete cessation of tumor growth with no obvious toxicity. Our findings give a new insight into the PSMA-targeted delivery of chemotherapeutics, and provide an opportunity for the development of novel active targeting drug delivery systems for PCa therapy.

INTRODUCTION

Prostate cancer (PCa) is the most prevalent cancer and remains the second-leading cause of cancer mortality and death affecting American males, in spite of recent advances in early diagnosis and surgical intervention.[1-3] Current standard therapies include radical prostatectomy, radiation, and adjuvant hormonal therapy. However,

these therapies are effective only in curing localized, low-grade PCa, the majority of patients initially diagnosed with localized PCa ultimately relapse.[4-8] Chemotherapy is the most widely used approach to combat advanced PCa, but its therapeutic effect is often unsatisfactory due to lack of specificity and toxicity.[8] Paclitaxel (PTX), a mitotic inhibitor, is the first line chemotherapy for PCa treatment. However, the clinical efficiency of PTX was greatly restricted by the significant side effects, which would be attributed to the non-specific biodistribution in the body.[9] Therefore, there is a critical need for target delivery of PCa therapeutic agents.

Prostate-specific membrane antigen (PSMA), also known as glutamate carboxypeptidase II, is a 100 KDa type II transmembrane glycosylated protein.[10] PSMA is overexpressed on the surface of nearly all PCa cells and the neovasculature of most solid malignant tumors.[11] More importantly, its expression level increases with cancer aggressiveness, recurrence and metastasis.[12] Although PSMA is expressed in some normal tissues, such as prostate, brain, small intestine and kidney,[13, 14] its expression level is 100 to 1000 fold higher in PCa cells compared to normal cells.[15, 16] The exceptionally high expression level of PSMA in PCa cells makes it becomes an excellent active target for the delivery of PCa therapeutic and imaging agents. Additionally, PSMA has internalization function via clathrin-coated pits and endocytosis, and this transport capability could be increased three fold upon ligand binding.[17, 18] DUPA belongs to a class of glutamate ureas and has high binding affinity with PSMA (K_i=8 nM).[19-21] After binding to DUPA, PSMA undergoes

internalization, releases DUPA into cytoplasm, and then returns to the cell membrane.[21, 22]

Based on the above considerations, we utilized DUPA as the targeting ligand to deliver PTX actively for treatment of PSMA expressing PCa. We hypothesized that conjugation of the targeting moiety DUPA will enhance the transport capability and selectivity of PTX to tumor cells via PSMA mediated endocytosis. Therefore, PTX-SS-DUPA was developed by conjugating DUPA with PTX, using a reduction-sensitive disulfide bond as a linkage to facilitate a rapid release of PTX in tumor cells (Scheme 1). An ester prodrug (PTX-DUPA) was synthesized as the non-sensitive conjugate. The tumor-targeting drug delivery and tumor-specific drug release would lead to improved antitumor efficacy and reduced toxicity.

Scheme 1. Redox-sensitive drug release mechanism of PTX-SS-DUPA triggered by GSH.

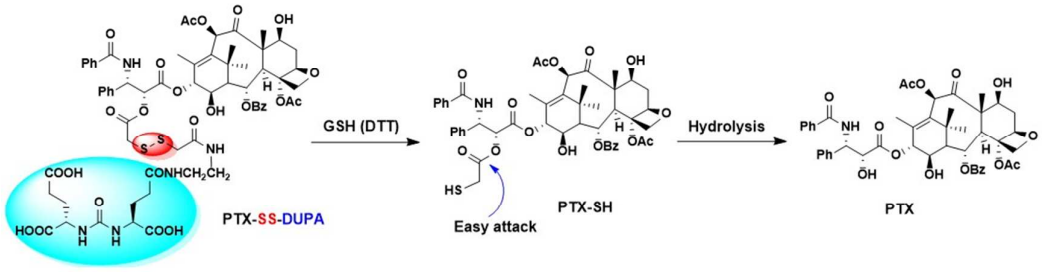

MATERIALS AND METHODS

Materials. PTX was obtained from Jingzhu Bio-technology Co. Ltd. (Nanjing, China). di-*tert*-butyl *L*-glutamate hydrochloride, DMAP and HATU were purchased

from Aladdin (Shanghai, China). F12K, 1640, DMEM media and fetal bovine serum (FBS) were obtained from Gibco BRL (Gaithersburg, MD, USA). Thiazolyl blue tetrazoliumbromide (MTT) and trypsin-EDTA were purchased from Sigma-Aldrich (St. Louis, MO, USA). Alexa Fluor® 488-labled anti-PSMA antibody were purchased from Abcam (Cambridge, MA, USA). DAPI was purchased from Beyotime (Shanghai, China). All other chemicals and reagents applied in this work were analytical or HPLC grade.

The PC-3, LNCaP, HK-2 and 22RV1 cell lines were obtained from the Cell Bank of the Chinese Academy of Sciences (Shanghai, China). 22RV1 and LNCaP human PCa cells were cultured in 1640 media, PC-3 and HK-2 cells were cultured in F12K and DMEM media respectively supplemented with 10% FBS, 100U mL^{-1} penicillin, and 100 μg mL^{-1} streptomycin. Cells were grown in a humidified 5% CO_2 atmosphere at 37 °C.

Synthesis of DUPA-conjugates.

5-benzyl 1-(*tert*-butyl)-(((*S*)-1,5-di-*tert*-butoxy-1,5-dioxopentan-2-yl)carbamoyl)-*L*-glutamate (1). To a solution of triphosgene (163 mg, 0.55 mmol) in DCM at -78 °C under argon, di-*tert*-butyl *L*-glutamate hydrochloride (488 mg, 1.65 mmol) and triethylamine (TEA, 0.5 mL) in DCM was added. After stirring for 2 h at -78 °C, a solution of 5-benzyl 1-(*tert*-butyl) *L*-glutamate hydrochloride (600 mg, 1.82 mmol) and TEA (0.3 mL) in DCM was added. The resulting mixture was stirred for 2 h at the same temperature and allowed to come to room temperature (rt). The reaction mixture

was stirred for additional 12 h and then quenched with 1 M HCl (30 mL), the organic phase was washed with brine, dried over Na_2SO_4, and concentrated. The residual oil was purified by silica column chromatography to yield **1** (778.68 mg, 81.55%). MS (ESI) *m/z*: 601.3 $[M+Na]^+$. ^1H NMR (600MHz, DMSO-d_6) δ 7.39 – 7.28 (m, 5H), 6.30 (m, *J* = 11.8, 8.3 Hz, 2H), 5.08 (s, 2H), 4.03 (qd, *J* = 8.7, 5.3 Hz, 2H), 2.46 – 2.31 (m, 2H), 2.28 – 2.14 (m, 2H), 1.99 – 1.81 (m, 2H), 1.70 (m, *J* = 51.2, 14.4, 8.7, 6.0 Hz, 2H), 1.41 – 1.27 (m, 27H).

(*S*)-5-(*tert*-butoxy)-4-(3-((*S*)-1,5-di-*tert*-butoxy-1,5-dioxopentan-2-yl)ureido)-5-oxopentanoic acid (2, DUPA(O^{t}Bu)-OH). To a stirred solution of compound **1** (300 mg, 0.52 mmol) in DCM, 10% Pd/C was added. The reaction mixture was vigorously stirred under a hydrogen atmosphere for 36 h at rt. The Pd/C was filtered off and wash with DCM, the organic phase was combined and evaporated under vacuum. The residue was purified using silica column chromatography to yield **2** (216.82 mg, 85.39%). MS (ESI) *m/z*: 511.3 $[M+Na]^+$. ^1H NMR (600MHz, DMSO-d_6) δ 12.13 (s, 1H), 6.29 (dd, *J* = 8.4, 3.6 Hz, 2H), 4.02 (m, *J* = 11.9, 8.6, 5.3 Hz, 2H), 2.31 – 2.15 (m, 4H), 1.87 (m, *J* = 15.2, 8.8, 6.1 Hz, 2H), 1.68 (m, *J* = 19.6, 14.4, 8.7, 6.1 Hz, 2H), 1.41 – 1.37 (m, 27H).

di-*tert*-butyl (((*S*)-5-((2-aminoethyl)amino)-1-(*tert*-butoxy)-1,5-dioxopentan-2-yl)carbamoyl)-*L*-glutamate (3). To a stirred solution of ethylenediamine (82.14 µL, 1.2 mmol) and DIPEA (143.2µL, 0.8mmol) in DCM under argon, a mixture of compound **2** (200 mg, 0.41 mmol) and HATU (187.07 mg, 0.48 mmol) in DCM was added. The resulting

mixture was stirred overnight. After completion of the reaction (monitored by TLC), the reaction mixture was concentrated and purified by silica column chromatography to yield **3** (171.87 mg, 63.29%). MS (ESI) *m/z*: 531.5 $[M+H]^+$. ^{1}H NMR (400MHz, DMSO-d_6) δ 8.03 (t, *J* = 5.6 Hz, 1H), 6.37 (dd, *J* = 8.4, 6.2 Hz, 2H), 4.01 (m, *J* = 34.1, 8.4, 5.2 Hz, 2H), 3.23 – 3.10 (m, 2H), 2.71 (t, *J* = 6.3 Hz, 2H), 2.32 – 2.15 (m, 2H), 2.13 (d, *J* = 7.9 Hz, 2H), 1.95 – 1.81 (m, 3H), 1.69 (m, *J* = 17.3, 14.7, 8.7, 6.5 Hz, 2H), 1.40 (d, *J* = 5.9 Hz, 27H), 1.33 – 1.22 (m, 1H).

2-((2-(((1*S*,2*R*)-1-benzamido-3-(((2a*R*,4*S*,4a*S*,6*R*,9*S*,11*S*,12*S*,12a*R*,12b*S*)-6,12b-diacetoxy-12-(benzoyloxy)-4,11-dihydroxy-4a,8,13,13-tetramethyl-5-oxo-2a,3,4,4a,5,6,9,10,11,12,12a,12b-dodecahydro-1*H*-7,11-methanocyclodeca[3,4]benzo[1,2-b]oxet-9-yl)oxy)-3-oxo-1-phenylpropan-2-yl)oxy)-2-oxoethyl)disulfanyl)acetic acid (4). A solution of 2,2'-disulfanediyldiacetic acid (366 mg, 2 mmol) in acetic anhydride (6 mL) was stirred at rt for 2 h under argon. Excessive acetic anhydride was removed with toluene under high vacuum at rt. The residue was reacted with PTX (1.71 g, 2 mmol) and DMAP (73.32 mg, 0.6 mmol) in DCM. The reaction mixture was stirred for 12 h under argon, and then concentrated. The residue was purified by silica gel chromatography to afford **4** (1.60 g, 78.66%). MS (ESI) *m/z*: 1016.5 $[M-H]^-$. ^{1}H NMR (600MHz, Chloroform-*d*) δ 8.14 – 8.06 (m, 2H), 7.81 – 7.76 (m, 2H), 7.66 – 7.59 (m, 1H), 7.55 – 7.46 (m, 3H), 7.41 (dq, *J* = 20.7, 7.7, 7.3 Hz, 7H), 7.33 – 7.27 (m, 1H), 6.27 (s, 1H), 6.19 – 6.08 (m, 1H), 5.96 (td, *J* = 8.5, 8.0, 4.5 Hz, 1H), 5.68 – 5.46 (m, 2H), 4.96 (dd, *J* = 9.5, 2.2 Hz, 1H), 4.39 (dd, *J* = 10.9, 6.7 Hz, 1H), 4.29 (dd, *J* = 8.5, 4.6 Hz, 1H), 4.16 (dd, *J* = 15.8, 8.6 Hz, 1H), 3.75 (d, *J* = 7.0 Hz, 1H), 3.71 –

3.59 (m, 2H), 3.55 – 3.47 (m, 2H), 2.58 – 2.49 (m, 1H), 2.43 (s, 2H), 2.41 (d, *J* = 23.6 Hz, 3H), 2.24 – 2.17 (m, 3H), 1.94 – 1.89 (m, 1H), 1.89 – 1.83 (m, 3H), 1.79 (s, 1H), 1.66 (s, 1H), 1.25 (s, 3H), 1.21 (s, 2H), 1.18 (s, 1H), 1.12 (d, *J* = 5.9 Hz, 3H).

1-((1*S*,2*R*)-1-benzamido-3-(((2a*R*,4*S*,4a*S*,6*R*,9*S*,11*S*,12*S*,12a*R*,12b*S*)-6,12b-diacetoxy-12-(benzoyloxy)-4,11-dihydroxy-4a,8,13,13-tetramethyl-5-oxo-2a,3,4,4a,5,6,9,10,11,12,12a,12b-dodecahydro-1*H*-7,11-methanocyclodeca[3,4]benzo[1,2-b]oxet-9-yl)oxy)-3-oxo-1-phenylpropan-2-yl) 13,17,19-tri-*tert*-butyl (13*S*,17*S*)-5,10,15-trioxo-2,3-dithia-6,9,14,16-tetraazanonadecane-1,13,17,19-tetracarboxylate (5). To a stirred mixture of compound **4** (509 mg, 0.5 mmol) and HATU (456mg, 1.2 mmol) in DCM under argon, compound **3** (270 mg, 0.5 mmol) and DIPEA (350 μL, 2 mmol) in DCM was added. The resulting mixture was stirred for 48 h. Upon completion (monitored by TLC), the reaction mixture was washed with brine (50 mL), dried over Na_2SO_4, and concentrated. The crude oil was purified by silica gel chromatography obtain **5** (469.97 mg, 61.45%). MS (ESI) *m/z*: 1553.1 $[M+Na]^+$.^{1}H NMR (600MHz, Chloroform-*d*) δ 8.31 (d, *J* = 8.4 Hz, 1H), 8.14 – 8.07 (m, 2H), 7.85 (dt, *J* = 7.2, 1.3 Hz, 2H), 7.66 – 7.59 (m, 2H), 7.56 – 7.48 (m, 4H), 7.48 – 7.41 (m, 1H), 7.37 (dt, *J* = 19.2, 7.7 Hz, 4H), 7.23 – 7.17 (m, 1H), 6.89 (t, *J* = 5.6 Hz, 1H), 6.28 (s, 1H), 6.16 – 6.06 (m, 1H), 5.86 (dd, *J* = 8.4, 6.2 Hz, 1H), 5.62 (t, *J* = 6.9 Hz, 3H), 5.47 (d, *J* = 6.2 Hz, 1H), 4.97 – 4.92 (m, 1H), 4.40 (dt, *J* = 11.8, 6.2 Hz, 1H), 4.27 (d, *J* = 8.5 Hz, 1H), 4.23 (td, *J* = 9.2, 8.3, 5.3 Hz, 2H), 4.16 (d, *J* = 8.5 Hz, 1H), 3.75 (d, *J* = 7.0 Hz, 1H), 3.71 – 3.53 (m, 2H), 3.45 – 3.34 (m, 3H), 3.30 (d, *J* = 14.2 Hz, 1H), 3.24 – 3.17 (m, 1H), 3.08 (s, 1H), 2.98 (d, *J* = 5.1 Hz, 1H), 2.55 – 2.46

(m, 1H), 2.39 (s, 3H), 2.31 (ddd, *J* = 11.4, 8.5, 5.0 Hz, 3H), 2.25 – 2.14 (m, 7H), 2.12 – 2.04 (m, 3H), 1.94 (s, 1H), 1.91 – 1.85 (m, 5H), 1.81 (dq, *J* = 17.5, 8.6, 8.0 Hz, 1H), 1.43 (d, *J* = 10.5 Hz, 27H), 1.38 (dd, *J* = 10.7, 5.3 Hz, 2H), 1.19 (s, 3H), 1.10 (s, 3H).

(3*S*,4*R*,19*S*,23*S*)-4-((((2a*R*,4*S*,4a*S*,6*R*,9*S*,11*S*,12*S*,12a*R*,12b*S*)-6,12b-diacetoxy-12-(benzoyloxy)-4,11-dihydroxy-4a,8,13,13-tetramethyl-5-oxo-2a,3,4,4a,5,6,9,10,11,12,12a,12b-dodecahydro-1*H*-7,11-methanocyclodeca[3,4]benzo[1,2-b]oxet-9-yl)oxy)carbonyl)-1,6,11,16,21-pentaoxo-1,3-diphenyl-5-oxa-8,9-dithia-2,12,15,20,22-pentaazapentacosane-19,23,25-tricarboxylic acid (6, PTX-SS-DUPA). To a stirred solution of compound **5** (300 mg, 0.2 mmol) in DCM under argon, TFA was added dropwise. The resulting reaction was stirred at rt for 1.5 h. The mixture was diluted in acetonitrile (ACN, 30 mL) and the solvent was evaporated under vacuum. The residue was purified by preparative reverse phase HPLC [solvent gradient: 20% A to 80% A in 50 min; A ACN; B 0.1% TFA; λ=227 nm]. The pure fractions were lyophilized for 24 h to yield PTX-SS-DUPA (108.51 mg, 40.66%). MS (ESI) *m/z*: 1362.4 $[M+H]^+$. ^{1}H NMR (600MHz, Methanol-d_4) δ 8.12 (d, *J* = 7.7 Hz, 1H), 8.01 (dd, *J* = 17.4, 7.8 Hz, 2H), 7.88 (dd, *J* = 9.3, 7.7 Hz, 2H), 7.78 (d, *J* = 7.7 Hz, 1H), 7.63 (m, 1H), 7.60 – 7.38 (m, 10H), 7.37 – 7.26 (m, 2H), 6.51 (d, *J* = 14.6 Hz, 1H), 5.93 (d, *J* = 4.9 Hz, 1H), 5.75 (d, *J* = 7.0 Hz, 1H), 5.60 (d, *J* = 5.0 Hz, 1H), 5.56 – 5.48 (m, 2H), 5.43 (dd, *J* = 13.8, 7.2 Hz, 1H), 5.36 (d, *J* = 6.8 Hz, 1H), 5.32 – 5.27 (m, 1H), 4.73 (d, *J* = 5.8 Hz, 1H), 4.43 – 4.37 (m, 1H), 4.35 – 4.28 (m, 3H), 4.16 (d, *J* = 12.1 Hz, 1H), 3.70 (d, *J* = 11.5 Hz, 1H), 3.67 – 3.62 (m, 1H), 3.41 (d, *J* = 3.5 Hz, 3H), 3.35 (s, 2H), 3.22-3.18 (m, 1H), 2.57 – 2.50 (m, 1H), 2.48 – 2.39 (m, 4H), 2.36 – 2.27 (m, 3H),

2.24 (s, 1H), 2.18 (s, 2H), 2.15 (d, *J* = 14.1 Hz, 1H), 2.13 -2.10 (m, 5H), 2.00 – 1.94 (m, 1H), 1.92 (m, 1H), 1.85 – 1.81 (m, 2H), 1.74 (s, 2H), 1.72 (d, *J* = 3.6 Hz, 3H), 1.33 (s, 2H), 1.29 (t, *J* = 7 Hz, 3H).

HPLC purity: 98.03%. [solvent gradient: 20% A to 80% A in 25 min; A ACN; B 10 mM NH_4OAc; λ=227 nm].

5-((1*S*,2*R*)-1-benzamido-3-(((2a*R*,4*S*,4a*S*,6*R*,9*S*,11*S*,12*S*,12a*R*,12b*S*)-6,12b-diacetoxy-12-(benzoyloxy)-4,11-dihydroxy-4a,8,13,13-tetramethyl-5-oxo-2a,3,4,4a,5,6,9,10,11,12,12a,12b-dodecahydro-1*H*-7,11-methanocyclodeca[3,4]benzo[1,2-*b*]oxet-9-yl)oxy)-3-oxo-1-phenylpropan-2-yl) 1-(*tert*-butyl) (((S)-1,5-di-*tert*-butoxy-1,5-dioxopentan-2-yl)carbamoyl)-*L*-glutamate (7). To a stirred solution of compound **2** (244.2 mg, 0.5 mmol), DCC (206.2 mg, 1 mmol) and DMAP (12.22 mg, 0.1 mmol) in DCM under argon, PTX (427.0 mg, 0.5 mmol) in DCM was added dropwise. The resulting mixture was stirred at rt for 48 h. Upon completion (monitored by TLC), the reaction mixture was filtered and concentrated. The crude oil was purified by silica gel column chromatography to obtain **7** (469.97 mg, 61.45%). MS (ESI) *m/z*: 1325.3 $[M+H]^+$. ^1H NMR (600MHz, Methanol-d_4) δ 8.15 – 8.10 (m, 2H), 7.86 – 7.81 (m, 2H), 7.68 (t, *J* = 7.4 Hz, 1H), 7.59 (t, *J* = 7.7 Hz, 2H), 7.56 – 7.41 (m, 8H), 6.46 (s, 1H), 6.10 (t, *J* = 9.3 Hz, 1H), 5.87 (d, *J* = 5.9 Hz, 1H), 5.65 (d, *J* = 7.1 Hz, 1H), 5.47 (d, *J* = 6.0 Hz, 1H), 4.59 (s, 4H), 4.40 – 4.32 (m, 2H), 4.21 – 4.15 (m, 3H), 4.10 (q, *J* = 7.1 Hz, 2H), 3.83 (d, *J* = 7.2 Hz, 1H), 2.61 – 2.54 (m, 1H), 2.49 (dt, *J* = 15.6, 7.2 Hz, 2H), 2.43 (s, 3H), 2.29 (q, *J* = 8.2 Hz, 2H), 2.26 – 2.17 (m, 2H), 2.17 (s, 3H), 2.15 – 2.08 (m, 1H), 2.01 (s, 4H), 1.95 (d, *J* = 1.5

Hz, 3H), 1.93 – 1.75 (m, 4H), 1.71 (d, *J* = 13.6 Hz, 1H), 1.66 (s, 3H), 1.60 (s, 2H), 1.45 (d, *J* = 2.1 Hz, 16H), 1.41 (s, 8H), 1.24-1.14 (t, *J* = 7.1 Hz, 4H).

(3*S*,4*R*,9*S*,13*S*)-4-((((2a*R*,4*S*,4a*S*,6*R*,9*S*,11*S*,12*S*,12a*R*,12b*S*)-6,12b-diacetoxy-12-(benzoyloxy)-4,11-dihydroxy-4a,8,13,13-tetramethyl-5-oxo-2a,3,4,4a,5,6,9,10,11,12,12a,12b-dodecahydro-1*H*-7,11-methanocyclodeca[3,4]benzo[1,2-*b*]oxet-9-yl)oxy)carbonyl)-1,6,11-trioxo-1,3-diphenyl-5-oxa-2,10,12-triazapentadecane-9,13,15-tricarboxylic acid (8, PTX-DUPA). PTX-DUPA was obtained as described for PTX-SS-DUPA starting from compound **7**. MS (ESI) *m/z*: 1156.4 $[M+H]^+$. ^{1}H NMR (600MHz, Methanol-d_4) δ 7.99 – 7.94 (m, 2H), 7.90 – 7.86 (m, 2H), 7.61 – 7.54 (m, 1H), 7.54 – 7.39 (m, 9H), 7.36 (d, *J* = 32.6 Hz, 1H), 7.29 (t, *J* = 7.4 Hz, 1H), 6.56 – 6.50 (m, 1H), 5.94 (d, *J* = 4.5 Hz, 1H), 5.59 – 5.50 (m, 2H), 5.36 (d, *J* = 6.7 Hz, 1H), 4.78 (s, 1H), 4.67 (s, 1H), 4.16 (d, *J* = 12.1 Hz, 1H), 3.91 – 3.81 (m, 2H), 3.45 (d, *J* = 6.8 Hz, 1H), 2.64 – 2.53 (m, 2H), 2.53 – 2.45 (m, 2H), 2.42 – 2.32 (m, 2H), 2.25 – 2.03 (m, 8H), 1.98 – 1.81 (m, 3H), 1.78 (s, 1H), 1.74 (d, *J* = 11.8 Hz, 6H), 1.62 (s, 3H), 1.34 (s, 3H), 1.30 (d, *J* = 10.2 Hz, 1H).

HPLC purity: 98.92%. [solvent gradient: 20% A to 80% A in 25 min; A ACN; B 10 mM NH_4OAc; λ=227 nm].

***In vitro* release of PTX from DUPA-drug Conjugates.**

The release of PTX from PTX-SS-DUPA and PTX-DUPA were studied in PBS (pH 7.4) containing 20% ethanol with 0 μM, 20 μM, 1 mM or 10 mM dithiothreitol (DTT), respectively. Briefly, DUPA conjugates (6 mg PTX equivalent) were incubated in 30 mL of release medium at 37 °C. At timed intervals, 0.2 mL of sample

was withdrawn, and the content of PTX, PTX-SS-DUPA and PTX-DUPA was determined by HPLC (Waters e2695 Separations Module and Waters 2489 UV-vis Detector on a reverse ODS Shiseido -C18 column (250 mm × 4.6 mm, 5 μm) with solvent gradient: 20% A to 80% A in 12 min; A ACN; B 10 mM NH_4OAc) at a flow rate of 1.0 mL min^{-1}. The UV detector was kept at 227 nm. Each experiment was repeated in triplicate, and the results were expressed by mean ± SD.

To investigate the release mechanism of PTX-SS-DUPA, a solution of PTX-SS-DUPA (200 μg mL^{-1}) in PBS (pH 7.4) containing 20% ethanol was incubated with 10 mM DTT. The efficiency of free PTX release from PTX-SS-DUPA was monitored by HPLC and Bruker microTOF-Q time-of-flight mass spectrometer.

***In vitro* cytotoxicity of DUPA-drug Conjugates.**

The *in vitro* cytotoxicity of PTX, PTX-SS-DUPA and PTX-DUPA was evaluated in PSMA-positive cell lines (22RV1 and LNCaP), a PSMA-negative cell line (PC-3) and a human proximal tubular cell line (HK-2) by the 3-(4,5-dimethylthiazol-2-yl)-2,5-diphenyl tetrazolium bromide (MTT) assay. Briefly, 22RV1 cells were seeded in 96-well plates at a density of 8000 cells per well. After 24 h incubation, cells were exposed to a series of PTX or its DUPA conjugates concentrations ranging from 2 to 500 nM at 37 °C for 48 h with or without 100-fold excess PMPA (a competitive inhibitor of PSMA). PTX, PTX-DUPA and PTX-SS-DUPA were dissolved in DMSO. The concentration of DMSO was no more than 0.05%. To assess cell viability, 20 μL of MTT (5 mg mL^{-1}) solution was added and incubated for 4 h at 37 °C. Then, the media was replaced with 200 μL of DMSO

to dissolve the formazan crystals formed by living cells. The absorbance was measured at 570 nm using a microplate reader (Varioskan Flash, Thermo Scientific, Waltham, MA, USA).

PSMA receptor expression and cellular uptake of PTX in PCa cells.

PSMA expression levels were determined by combined immunocytostaining and flow cytometry. For immunocytostaining analysis, cells were planted on sterile cover slips placed in a 24-well plate at a density of 50,000 cells per well, and cells were allowed to attach for 24 h. The cells were then washed with PBS thrice, followed by fixation with 4% paraformaldehyde for 20 min. Fixed cells were stained using Alexa Fluor 488 labeled monoclonal anti-PSMA antibody (1:100 dilution; Abcam, Cambridge, MA, USA) overnight at 4 ℃. Cells were counter-stained with DAPI for nuclear recognition prior to imaging on the confocal laser scanning microscopy (C2SI, Nikon Corp., Tokyo, Japan). For flow cytometry analysis, 100,000 cells were incubated with Alexa Fluor 488 labeled monoclonal anti-PSMA antibody (6 μg mL^{-1}) for 15 min at 25 °C. Following the incubation, the cells were washed three times with PBS, gently dissociated from the wells with trypsin, and re-suspended in 0.4 mL PBS. The fluorescence intensity was analyzed on a flow cytometer (Becton Dickinson Immunocytochemistry Systems, San Jose, CA, USA).

For cellular uptake studies, 22RV1 cells were grown on 12-well plate at a density of 150,000 cells per well and cultured for 24 h. Cells were exposed to PTX or its DUPA conjugates solution (1 μM, dissolved in 0.05% DMSO) at 37 °C for 1, 4 and 8 h with or without 100-fold excess PMPA. The samples were collected and subjected to

ultrasonication. PTX concentration was determined by the UPLC-MS/MS method. A BCA protein assay kit was used to determine the protein content in cell lysates, and the cellular uptake of PTX was corrected to per gram protein. Each experiment was repeated three times.

Animals and tumor xenograft model.

Athymic nude BALB/c male mice (23-26 g) were purchased from Vital River Laboratory Animal Technology Co. Ltd. (Beijing, China). All animal studies were carried out under Institutional Animal Care and Use Committee-approved protocols of Shenyang Pharmaceutical University. The tumor xenograft models were established by injecting 5×10^6 PSMA-expressing 22RV1 cells in 50% Matrigel (BD Biosciences, SanJose, CA) into the armpit region of mice.

Tissue distribution study

To determine the tissue distribution of PTX and PTX-SS-DUPA, we used mouse xenografts bearing 22RV1 tumors. Mice with subcutaneous tumors of ~100-150 mm^3 were administered through tail vein injection of PTX, PTX-SS-DUPA or PTX-DUPA solution at an equivalent PTX dose of 10 mg kg^{-1}. At 24 h post-treatment, tumor, heart, liver, spleen, lung and kidney were harvested. UPLC-MS/MS was used to measure the concentration of PTX in tissue samples.

***In vivo* anticancer efficacy of DUPA-drug Conjugates**

Mice bearing 22RV1 tumors were utilized to investigate the *in vivo* antitumor activity of PTX and its DUPA conjugates. When the average tumor volume reached ~100 mm^3, the mice were randomly assigned to 4 groups (n=5 per group): (1) saline

(the control group), (2) free PTX solution, (3) PTX-SS-DUPA solution, (4) PTX-DUPA solution. These preparations were administrated through tail veins every other day for five times at an equivalent PTX dose of 10 mg kg^{-1}. Tumor volume and body weight were recorded. Mice were sacrificed 24 h after the final injection, and blood was collected from the retro-orbital sinus. The serum levels of blood urea nitrogen (BUN), creatinine, aspartate transaminase (AST), alanine transaminase (ALT) and uric acid were determined to assess hepatic and renal function. The serum prostate specific antigen (PSA) levels were determined by an ELISA kit (Cusabio Biotech, Wuhan, China) in accordance with the manufacturer's protocols.

The tumors and major organs (heart, liver, spleen, lung, kidney) were harvested and sectioned for further pathological assessment. Tumor cell apoptosis was investigated by the terminal deoxynucleotidyl transferase-mediated dUTP nick end-labeling (TUNEL) assay using an apoptosis detection kit (KeyGen Biotech, Nanjing, China) according to the manufacturer's instructions. The nuclei of tumor slices were stained by DAPI. All stained samples were observed with a confocal laser scanning microscopy (C2SI, Nikon Corp., Tokyo, Japan). The formalin-embedded tissues were stained with hematoxylin and eosin (H&E) to assay the systematic toxicity.

Statistical analysis.

Data are expressed as mean ± SD. A one-way ANOVA was used to determine the significance in the experiments. Statistical differences were significant at $P < 0.05$ and highly significant at $P < 0.01$.

RESULTS AND DISCUSSIONS

Design and synthesis of DUPA-conjugates.

The synthesis of *tert*-butyl protected DUPA (2, DUPA(O^{t}Bu)-OH) was shown in Scheme **2**. Commercially available *γ*-benzoylated glutamic acid was treated with triphosgene in DCM containing TEA at 78 °C for 2 h followed by addition of *tert*-butyl-protected glutamic acid to obtain **1**. Deprotection of the benzyl group of **1** obtained DUPA(O^{t}Bu)-OH (2). The structure of compound **1** and **2** was confirmed by ^{1}H NMR (Supporting Information, Figure S1, S2).

Scheme 2

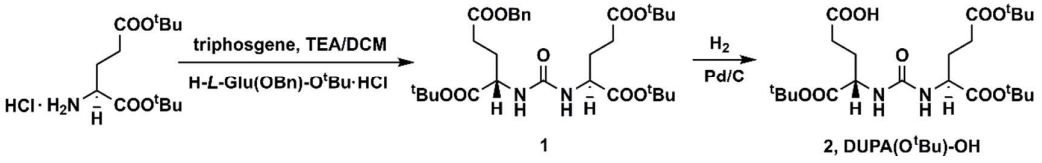

The synthesis of the desired PTX-SS-DUPA conjugate **6** was shown in Scheme 3. The carboxylic acid **2** was coupled with ethylenediamine to obtain **3** in the presence of HATU and DIPEA in DCM. Dithiodiglycolic acid was converted to the corresponding anhydride using acetic anhydride as dehydration agent. The residue was reacted with PTX, using DMAP as catalyst, to obtain **4**. The amine **3** was coupled with carboxylic acid **4** in the presence of HATU and DIPEA in DCM to produce 5. The ^{1}H NMR spectrums of compound **3-5** were illustrated in Figure S3-5, the mass spectrum of **5** was illustrated in Figure S6. Deprotection of the *tert*-butyl group of **5** obtained the target compound PTX-SS-DUPA (**6**). The final product was purified

using preparative reverse phase HPLC and characterized by ^{1}H NMR and HRMS (Figure S7, 8).

Scheme 4 shows the synthesis of ester prodrug PTX-DUPA (**8**). The carboxylic acid **2** was coupled with PTX in the presence of DCC and DMAP to produce **7** which was confirmed by mass spectrometry and ^{1}H NMR (Figure S9, S10). Deprotection of the *tert*-butyl group of **7** obtained the ester prodrug PTX-DUPA (**8**). The final product was purified using preparative reverse phase HPLC and characterized by ^{1}H NMR and HRMS (Figure S11, 12). The octanol-water distribution coefficients (log P) of DUPA-SS-PTX and PTX-DUPA was 1.199 and 2.674, respectively. The hydrophilicity of DUPA-SS-PTX and PTX-DUPA was slightly increased due to the introduction of DUPA moiety.

Scheme 3

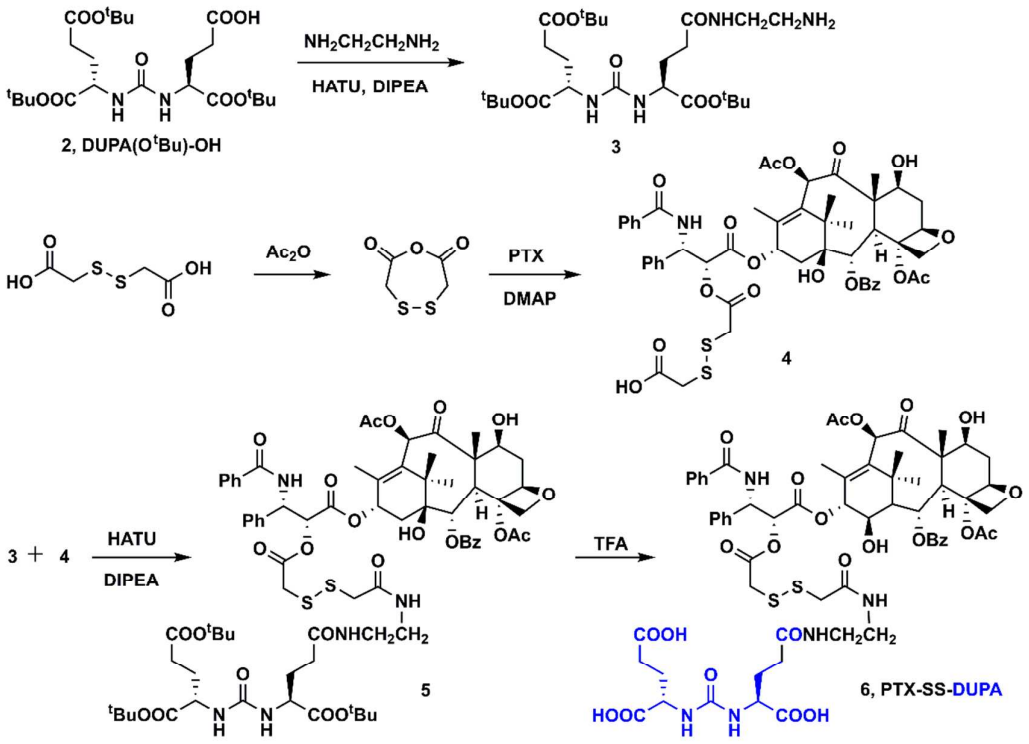
COO^{t}Bu
COOH
^{t}BuOOC
COO^{t}Bu
2, DUPA(O^{t}Bu)-OH
$NH_2CH_2CH_2NH_2$
HATU, DIPEA
CONHCH$_2$CH$_2$NH$_2$
3
Ac_2O
PTX
DMAP
4
3 + 4
HATU
DIPEA
5
TFA
6, PTX-SS-DUPA

Scheme 4

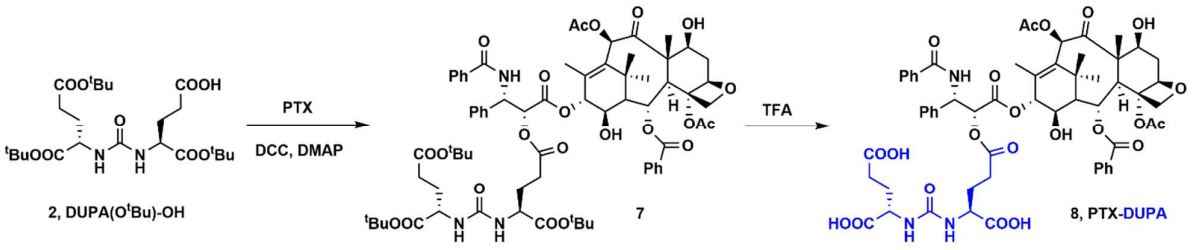

***In vitro* release of PTX from DUPA-drug Conjugates.**

The *in vitro* drug release profiles of PTX-DUPA and PTX-SS-DUPA were investigated using DTT (a prevailing GSH simulant) containing release media [23, 24]. As shown in Figure 1 A, less than 20% of PTX was released from PTX-SS-DUPA within 24 h in blank PBS (pH 7.4) and PBS containing 20 μM DTT, and about 80% of PTX was released within 4 h in the presence of 1 mM and 10 mM DTT. By contrast, there was negligible PTX (<2.1%) released from PTX-DUPA after 24 h incubation in the presence or absence of 10 mM DTT (Figure 1 B). These results suggested that the drug release from ester prodrug (PTX-DUPA) was extremely slow, and PTX-SS-DUPA had a remarkable redox-responsive drug release. In addition, the results indicated that PTX-SS-DUPA conjugate would remain stable in circulation but release PTX following disulfide reduction in tumor cell.[25] The rapid and differential drug release within tumor cells would lead to enhanced antitumor efficacy and reduced toxicity.[24]

To investigate the mechanism of DTT-triggered drug release, the change of molecule weight was analyzed by HPLC and HRMS. Figure 1 C indicated that all PTX-SS-DUPA prodrugs were reduced within 2 h after addition of DTT. The

breakage of the disulfide bond generated a thiol-containing intermediate (PTX-SH, confirmed by HRMS) which would eventually release free PTX (Scheme 1).

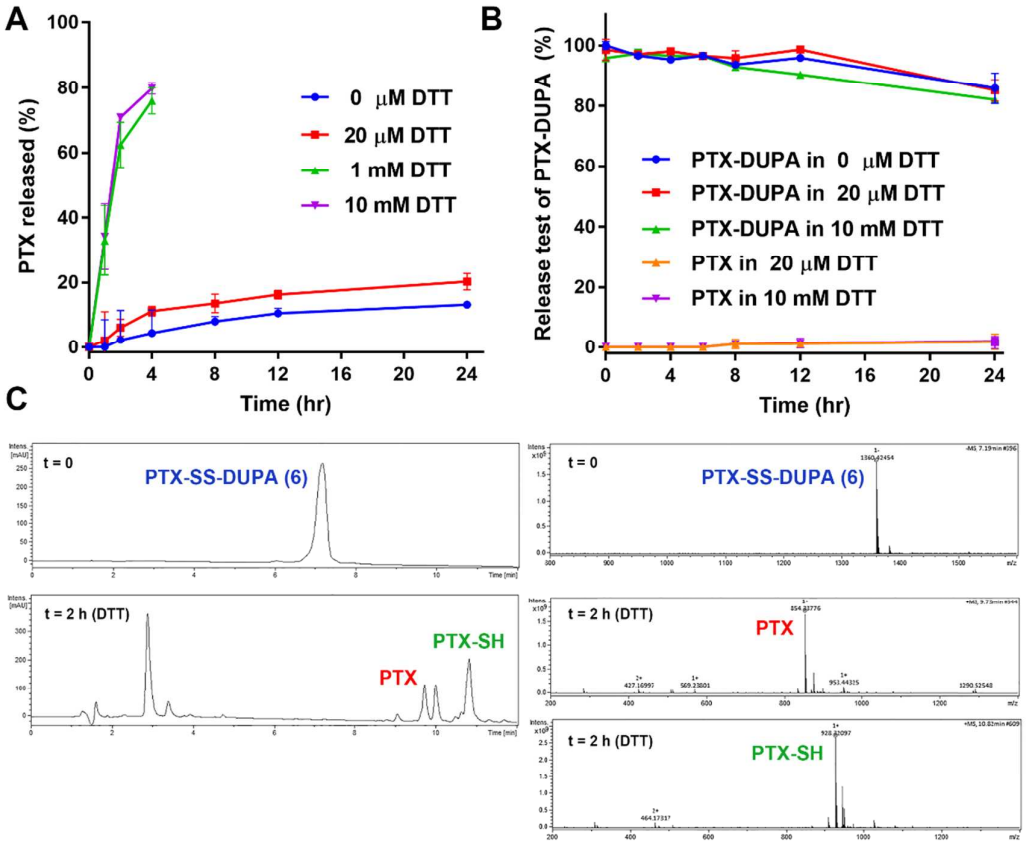

Figure 1. *In vitro* release of PTX from prodrugs. (A) Release profiles of PTX from PTX-SS-DUPA with 0 μM, 20 μM, 1 mM or 10 mM DTT in PBS (pH 7.4) (n = 3). (B) Release profiles of PTX from PTX-DUPA and the content of PTX-DUPA in release medium. (C) HPLC spectra of PTX-SS-DUPA with 10 mM DTT at 0 and 2 h. HRMS spectra of PTX-SS-DUPA, PTX-SH, and PTX.

***In vitro* cytotoxicity of DUPA-drug Conjugates.**

The *in vitro* cytotoxicity of PTX-DUPA and PTX-SS-DUPA was evaluated in PSMA-positive cell lines (22RV1 and LNCaP), a PSMA-negative cell line (PC-3) and

a human proximal tubular cell line (HK-2) using MTT assay. As shown in Figure 2 A and S13 A, cell viability decreased with increasing concentrations of PTX and PTX-SS-DUPA in PSMA expressing 22RV1 and LNCaP cells. PTX-SS-DUPA (IC_{50}= 121.1 nM) was less potent than PTX (IC_{50}=14.25 nM) in 22RV1 cells, possibly because of the delayed release of PTX (Figure 2 C). The high efficacy of PTX-SS-DUPA was quantitatively inhibited by excess PMPA, which suggested that cytotoxicity required PSMA receptors.[21] By contrast, PTX-DUPA (IC_{50}=563.3 nM) exhibited poor cytotoxicity within the studied range of drug concentrations, due to the extremely slow hydrolysis rate of PTX. In addition, PMPA alone cause no cytotoxicity even at the concentration of 30 μM (cell viability=96.69%), suggesting PMPA did not affect the cell function. As shown in Figure 2 B and S13 B, PTX-SS-DUPA exhibited inferior cytotoxicity in PSMA negative PC-3 and HK-2 cells, showing no significant difference compared with PTX-DUPA at the concentration of 500 nM. The results further suggested cell killing required PSMA receptors and rapid release of active PTX moiety within tumor cells.

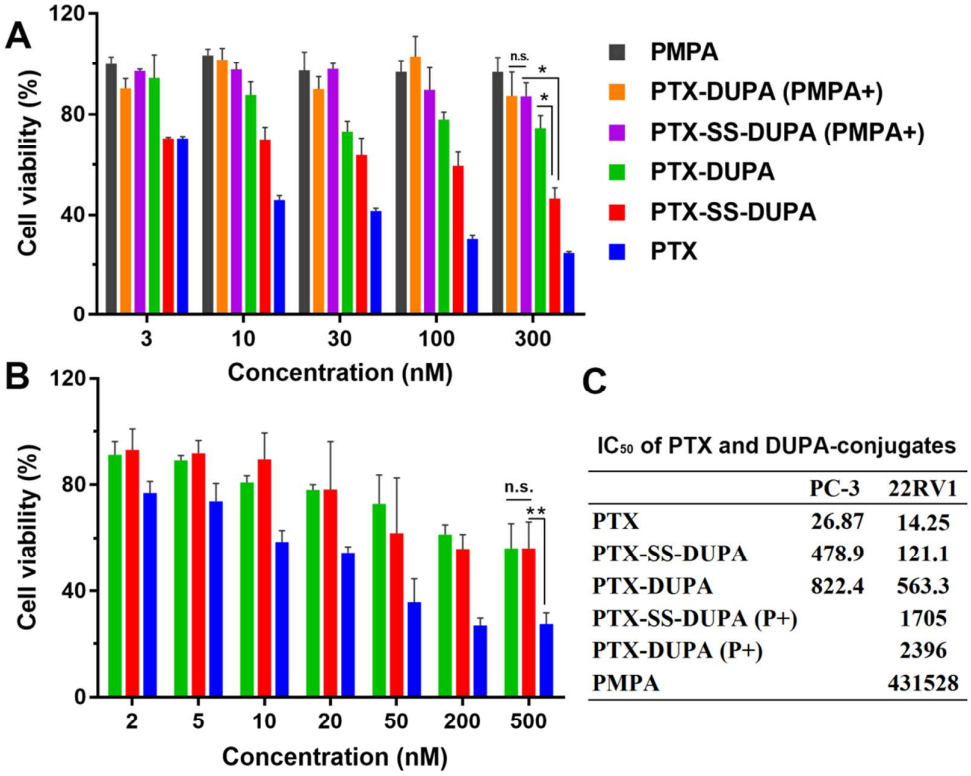

IC_{50} of PTX and DUPA-conjugates

	PC-3	22RV1
PTX	26.87	14.25
PTX-SS-DUPA	478.9	121.1
PTX-DUPA	822.4	563.3
PTX-SS-DUPA (P+)		1705
PTX-DUPA (P+)		2396
PMPA		431528

Figure 2. *In vitro* cytotoxicity of PTX and its DUPA conjugates in 22RV1 and PC-3 cells. (A) Cytotoxicity of PTX, PTX-SS-DUPA, PTX-DUPA, PMPA (100-fold excess), and cytotoxicity of DUPA-drug conjugates in the presence of 100-fold excess PMPA in 22RV1 cells. (B) Cytotoxicity of PTX, PTX-SS-DUPA and PTX-DUPA in PC-3 cells. (C) IC_{50} of PTX, PTX-SS-DUPA and PTX-DUPA in PCa cells. The data are presented as means ± SD, P values: *P < 0.05, **P < 0.01.

PSMA expression and cellular uptake of PTX in PCa cells.

PSMA receptor expression of human PCa cell lines 22RV1 and PC-3 was determined by combined immunocytostaining and flow cytometry. As shown in Figure 3 A, PSMA receptor was robustly expressed by 22RV1 cells and complete

absence of staining observed in PC-3 cells (green, PSMA receptor; blue, nucleus). For flow cytometry, human PCa cell lines 22RV1 and PC-3 were stained with Alexa Fluor 488 labeled monoclonal anti-PSMA antibody. As shown in Figure 3 B, expression of a high level of PSMA was observed in the 22RV1 cells, whereas PC-3 cells lacked PSMA expression (Cyan, unstained cells; red, cells with antibody).

To confirm the contribution of PSMA to the transport of the targeted DUPA-drug conjugates, PSMA-positive 22RV1 cells were used to evaluate the cellular uptake efficiency. PTX concentration in PCa cells was determined by UPLC-MS/MS. As shown in Figure 3 C, the intracellular concentration of PTX increased with time after incubation with free PTX and its DUPA conjugates in 22RV1 cells. The PTX concentration in cells derived from PTX-SS-DUPA and free PTX solution was markedly higher than PTX-DUPA. Besides, the cellular uptake of PTX-SS-DUPA was quantitatively inhibited by excess PMPA, indicating PMPA effectively prevented PTX-SS-DUPA from binding to PSMA, thereby blocking the cellular uptake of PTX-SS-DUPA. In the same time, the higher intracellular concentration of PTX derived from PTX-SS-DUPA suggested it could release active PTX molecules rapidly following internalization into the tumor cells.

By contrast, the PTX concentration in 22RV1 cells of free PTX solution did not change in the absence of excess PMPA, indicating that the PTX cellular uptake occur through passive diffusion into the cell but not PSMA mediated internalization. The PTX concentration in 22RV1 cells of PTX-DUPA was poor because of slow drug release from ester prodrug, which may lead to poor antitumor efficiency.

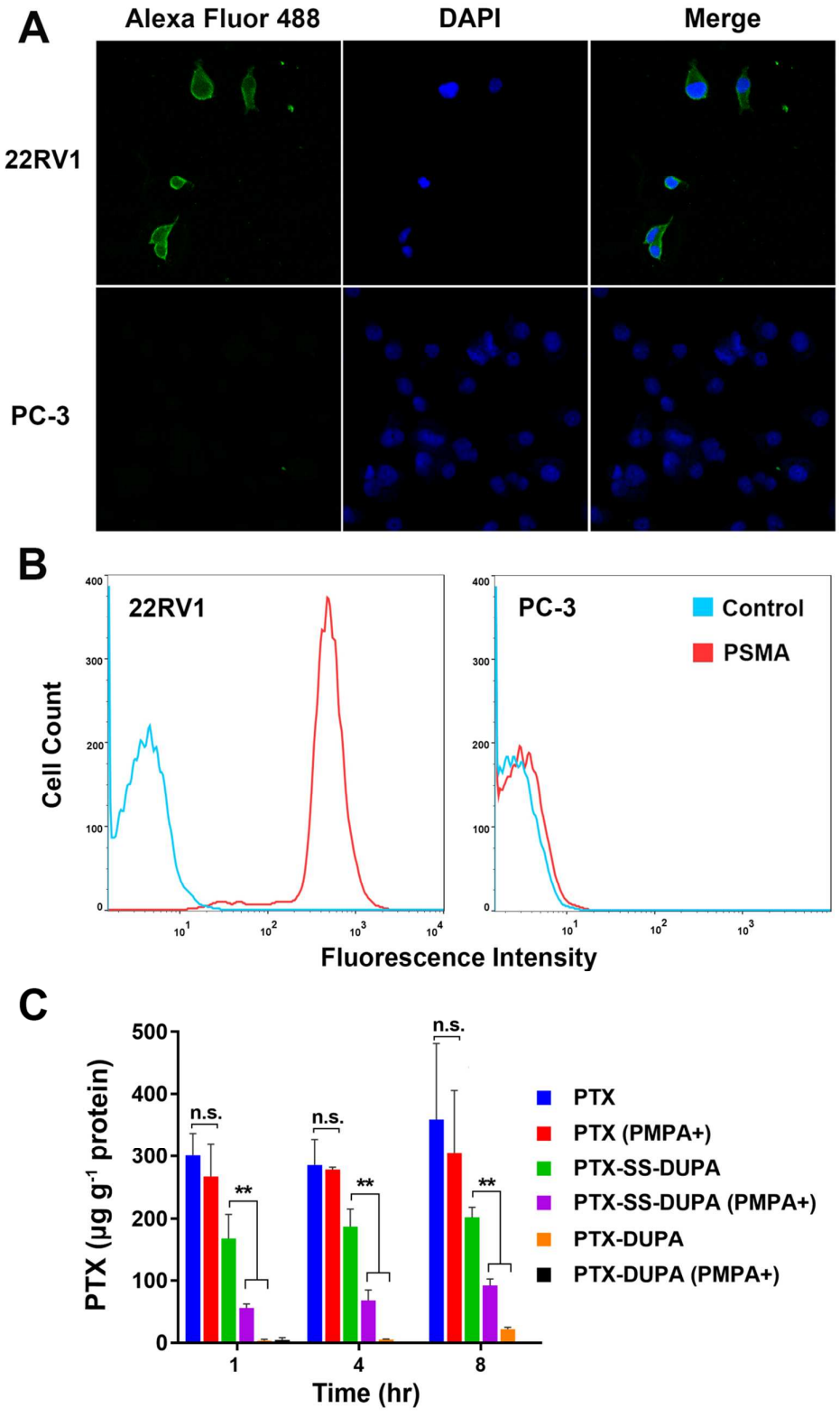

Figure 3. Expression of PSMA and cellular uptake of PTX in 22RV1 and PC-3 cells.

(A) Expression of PSMA demonstrated by confocal fluorescent microscopy in 22RV1 and PC-3 cells (green, PSMA receptor; blue, nucleus). (B) Quantitative expression of PSMA in 22RV1 cells investigated by flow cytometry after incubation of cells with anti-PSMA-Alexa Fluor 488 conjugate (Cyan, unstained cells, control; red, cells with antibody, PSMA). (C) Cellular uptake of PTX in 22RV1 cells (n=3). The data are presented as means ± SD, P values: **P < 0.01.

Tissue distribution study

In view of the favorable cellular uptake of PTX-SS-DUPA in PCa cells, we further investigated the tissue distribution of PTX-SS-DUPA and PTX-DUPA in mice xenograft models bearing 22RV1 tumors in comparison with PTX solution. The content of PTX in major organs was determined using UPLC-MS/MS, and illustrated in Figure 4 A and B. At 24 h after injection, the accumulation of PTX in tumor of PTX-SS-DUPA group was less than that of PTX solution. However, PTX solution did not show tumor targeting with high drug contents in lung (6.35 μg g^{-1}), which will lead to toxicity in normal organs. The content of PTX in tumors of PTX-SS-DUPA group was higher than that in other organs. The potential value of cancer targeting by PTX-SS-DUPA would be derived from its lack of toxicity in other organs, which might make it a less toxic anticancer drug than PTX. There was negligible PTX (0.01 μg g^{-1}) detected in tumors of PTX-DUPA group due to extremely slow release rate of PTX. The PSMA-targeting moiety DUPA significantly changed the biodistribution

and leaded to much higher accumulation of drug in tumor compared with other major organs due to the selective uptake by PCa cells.

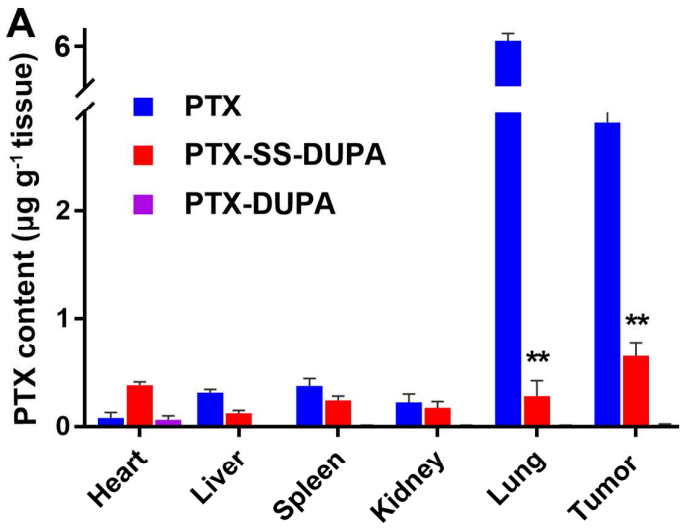

B **PTX content in tissues (μg g^{-1} tissue)**

Tissue \ Group	PTX	PTX-SS-DUPA	PTX-DUPA
Heart	0.08 ± 0.05	0.38 ± 0.03	0.06 ± 0.04
Liver	0.31 ± 0.03	0.12 ± 0.03	-
Spleen	0.37 ± 0.07	0.24 ± 0.04	-
Lung	6.35 ± 0.46	0.28 ± 0.14	-
Kidney	0.22 ± 0.08	0.17 ± 0.06	-
Tumor	2.81 ± 0.62	0.65 ± 0.13	0.01 ± 0.01

Figure 4. The content of PTX in major organs and tumor of PTX and its DUPA conjugate. (A) The content of PTX in major organs and tumor of PTX, PTX-SS-DUPA and PTX-DUPA group on 22RV1 tumor xenografts. (B) PTX content in major tissues of PTX, PTX-SS-DUPA and PTX-DUPA group determined by UPLC-MS/MS.

***In vivo* anticancer efficacy of DUPA-drug Conjugates.**

Based on the favorable anti-tumor effect of PTX-SS-DUPA *in vitro*, we further investigated the *in vivo* anti-tumor activities of PTX-SS-DUPA in mice xenograft models bearing 22RV1 tumors. PTX, PTX-SS-DUPA or PTX-DUPA were injected intravenously into mice every 2 days, with a total of 5 injections. As shown in Figure 5 A and B, PTX-DUPA exhibited a moderate anti-tumor effect as compared to the PTX group and PTX-SS-DUPA group, which may due to its slow release rate of active PTX molecular and low intracellular PTX concentration. In contrast, the mice treated with PTX-SS-DUPA displayed a significant decrease in tumor volume, showing no significant difference compared with PTX. (Figure 5 B, D). PSA levels in mice were determined on day 10, and PTX-SS-DUPA treated mice had a significant reduction in PSA levels (Figure 5 C). The potent antitumor efficacy of PTX-SS-DUPA could be attributed to the efficient cellular uptake mediated by PSMA and on-demand release of active PTX molecules in tumor cells, which will result in potent chemotherapeutic efficacy with decreased off-target toxicities compared with PTX.[21]

The TUNEL assay was used to evaluate if apoptosis is induced in tumor cells by PTX, PTX-SS-DUPA and PTX-DUPA treatment (Figure 5 E). A robust and significant increase in cell apoptosis was observed in tumor samples treated with PTX and PTX-SS-DUPA, as compared to both saline and PTX-DUPA group. Additionally, there was no significant change observed in body weight or in the hematological parameters between treated and control groups (Figure 6 A, B). Furthermore, no noticeable histological abnormalities were observed in H&E staining of major organ

sections, indicating that the DUPA conjugates treatments were well tolerated. This confirms that the PTX-SS-DUPA conjugate has potent antitumor activity and no treatment-induced toxicity (Figure 7). The superior safety of PTX-SS-DUPA could be attributed to that the targeting moiety DUPA enhances the transport capability and selectivity of PTX to tumor cells via PSMA mediated endocytosis.[8, 20, 26, 27] Besides, DUPA were conjugated with PTX via a disulfide bond, which facilitates the rapid and differential drug release in tumor cells.[24, 28-30]

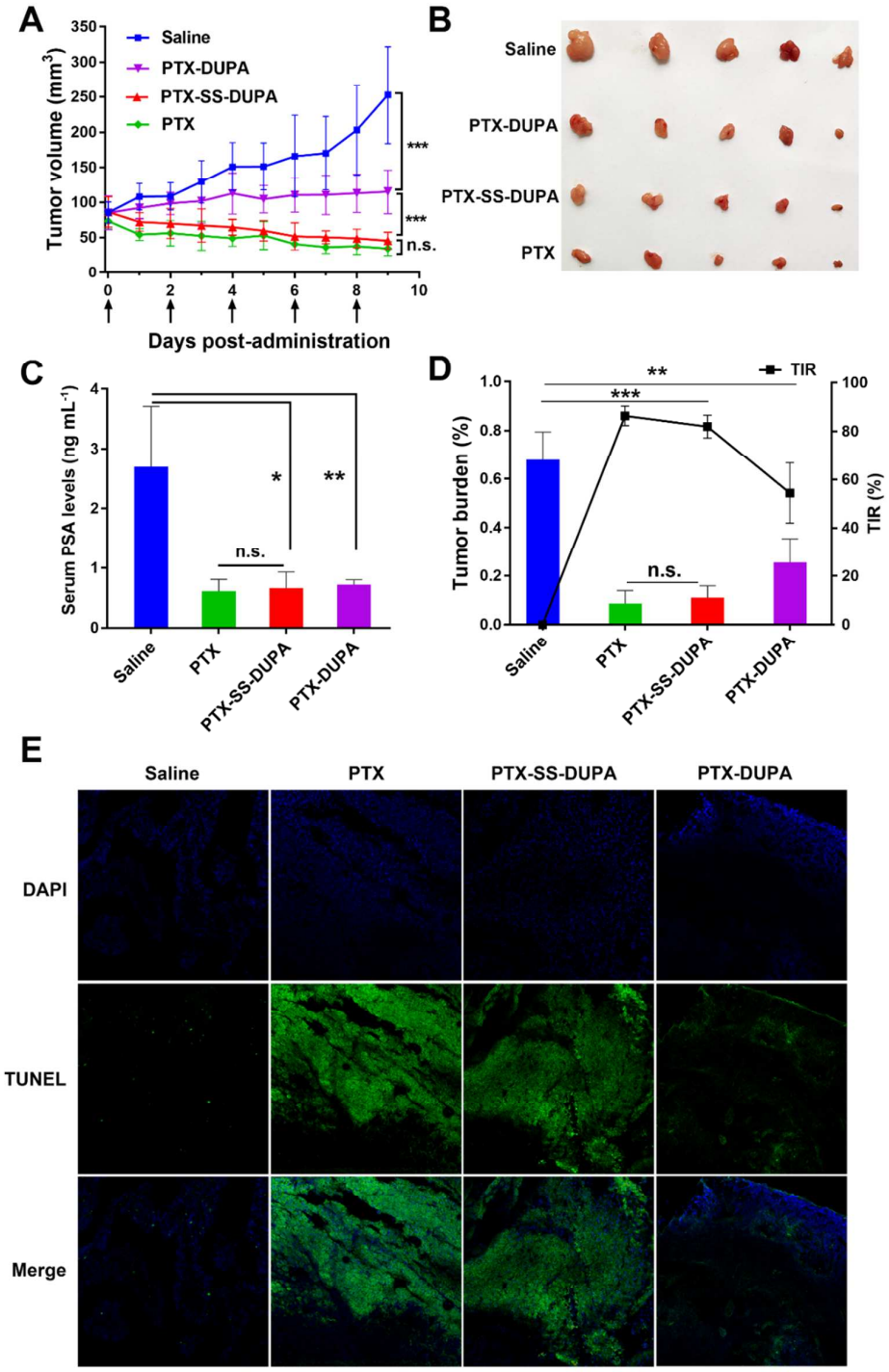

Figure 5. *In vivo* antitumor efficiency of PTX, PTX-SS-DUPA and PTX-DUPA on 22RV1 tumor xenografts. (A) The tumor volume after intravenous administration of saline, PTX, PTX-SS-DUPA or PTX-DUPA (n=5). (B) The morphology of dissected tumors from 22RV1 tumor-bearing mice of different groups at the end of tests (n=5).

(C) Serum PSA levels in 22RV1 tumor-bearing mice determined on day 10 after the treatment by ELISA. (D) Tumor burden (the weight of tumor was divided by the average body weight of mice) and tumor inhibition rate (TIR) of various groups. (E) TUNEL assay images of tumor specimens treated with different preparations. The data are presented as means ± SD, P values: *P < 0.05, **P < 0.01, *** P < 0.001.

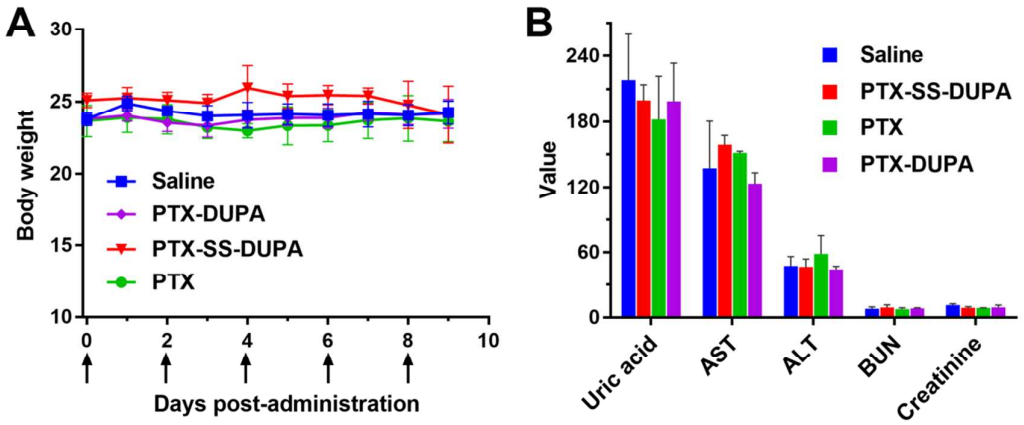

Figure 6. Body weight and the hematological parameters obtained in treated and control groups. (A) Body weight changes after intravenous administration of saline, PTX, PTX-SS-DUPA or PTX-DUPA (n=5). (B) Hepatic and renal function indicators of mice bearing 22RV1 tumor xenografts after treatment (n=5).

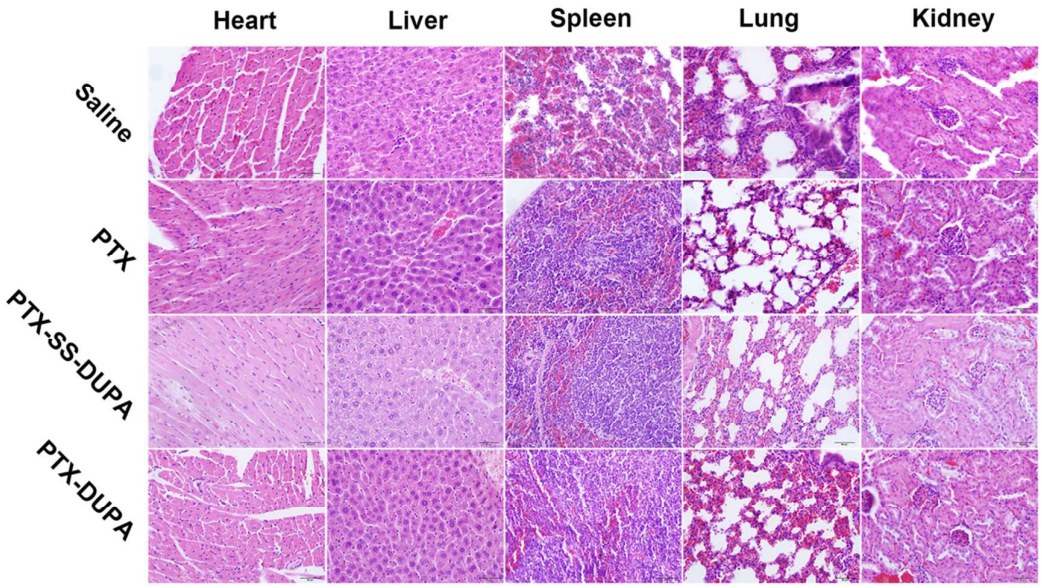

Figure 7. Light microscopy images of H&E staining major organs after the treatment of different formulations.

CONCLUSION

To develop advanced PSMA-targeted PCa therapy, we herein report DUPA conjugation of a mitotic inhibitor PTX as an effective approach to safely and selectively deliver PTX to PCa cells. The PSMA-targeting moiety DUPA was conjugated with the potent, cytotoxic mitotic inhibitor PTX through a disulfide linkage for rapid and differential drug release (PTX-SS-DUPA). An ester prodrug (PTX-DUPA) was used as the non-sensitive control. Experimental results indicated that the targeting moiety DUPA enhanced the transport capability and selectivity of PTX to tumor cells via PSMA mediated endocytosis.[21, 23, 27] PTX-SS-DUPA conjugate remained stable in circulation but release PTX following disulfide reduction within PCa cells. As a result of efficient cellular uptake and rapid release of active

PTX molecules in tumor cells, PTX-SS-DUPA exhibited an IC_{50} in the low nanomolar range in PSMA expressing cell lines and induced a complete cessation of tumor growth with no obvious toxicity after the last treatment. The PSMA-targeted conjugate with redox-responsive drug release provides a great potential for the development of novel active targeting drug delivery systems for PCa therapy.

■ ASSOCIATED CONTENT

* S Supporting Information

The Supporting Information is available free of charge on the ACS Publications website at

^{1}H NMR and mass spectrums of intermediate and targeting products; *In vitro* cytotoxicity of PTX and its DUPA conjugates in LNCaP and HK-2 cells.

■ AUTHOR INFORMATION

Corresponding Authors

*Phone: +86-24-23986325; E-mail: wangyjspu@163.com

*Phone: +86-24-23986411; E-mail: xuyoujun@syphu.edu.cn

*Phone: +86-24-23986321; E-mail: hezhonggui@vip.163.com

Notes

The authors declare no competing financial interest.

REFERENCES

1. Zhang, E.; Zhang, C.; Su, Y.; Cheng, T.; Shi, C. Newly developed strategies for multifunctional mitochondria-targeted agents in cancer therapy. *Drug Discovery Today* **2011,** *16*, (3-4), 140-146.

2. Xiang, B.; Dong, D. W.; Shi, N. Q.; Gao, W.; Yang, Z. Z.; Cui, Y.; Cao, D. Y.; Qi, X. R. PSA-responsive

and PSMA-mediated multifunctional liposomes for targeted therapy of PCa. *Biomaterials* **2013,** *34*, (28), 6976-6991.

3. Wang, X.; Huang, S. S.; Heston, W. D. W.; Guo, H.; Wang, B. C.; Basilion, J. P. Development of Targeted Near-Infrared Imaging Agents for Prostate Cancer. *Molecular Cancer Therapeutics* **2014,** *13*, (11), 2595-2606.

4. Ha, D.; Bing, S. J.; Ahn, G.; Kim, J.; Cho, J.; Kim, A.; Herath, K. H.; Yu, H. S.; Jo, S. A.; Cho, I. H.; Jee, Y. Blocking glutamate carboxypeptidase II inhibits glutamate excitotoxicity and regulates immune responses in experimental autoimmune encephalomyelitis. *The FEBS journal* **2016,** *283*, (18), 3438-3456.

5. Barve, A.; Jin, W.; Cheng, K. Prostate cancer relevant antigens and enzymes for targeted drug delivery. *Journal of Controlled Release* **2014,** *187*, 118-132.

6. Ristau, B. T.; O'Keefe, D. S.; Bacich, D. J. The prostate-specific membrane antigen: Lessons and current clinical implications from 20 years of research. *Urologic Oncology: Seminars and Original Investigations* **2014,** *32*, (3), 272-279.

7. Roy J, N. T., Kanduluru AK, Venkatesh C. DUPA Conjugation of a Cytotoxic Indenoisoquinoline Topoisomerase I Inhibitor for Selective Prostate Cancer Cell Targeting. *J Med Chem* **2015,** *58*, 3094-3103.

8. Barve, A.; Jin, W.; Cheng, K. Prostate cancer relevant antigens and enzymes for targeted drug delivery. *Journal of controlled release : official journal of the Controlled Release Society* **2014,** *187*, 118-132.

9. Zhang, Z.; Mei, L.; Feng, S.-S. Paclitaxel drug delivery systems. *Expert Opinion on Drug Delivery* **2013,** *10*, (3), 325-340.

10. Ahmadzadehfar, H.; Rahbar, K.; Kurpig, S.; Bogemann, M.; Claesener, M.; Eppard, E.; Gartner, F.; Rogenhofer, S.; Schafers, M.; Essler, M. Early side effects and first results of radioligand therapy with (177)Lu-DKFZ-617 PSMA of castrate-resistant metastatic PCa: a two-centre study. *EJNMMI research* **2015,** *5*, (1), 1-8.

11. Chang, S. S.; O'Keefe, D. S.; Bacich, D. J.; Reuter, V. E.; Heston, W. D.; Gaudin, P. B. Prostate-specific membrane antigen is produced in tumor-associated neovasculature. *Clinical Cancer Research An Official Journal of the American Association for Cancer Research* **1999,** *5*, (10), 2674.

12. Ross, J. S.; Sheehan, C. E.; Fisher, H. A.; Jr, K. R.; Kaur, P.; Gray, K.; Webb, I.; Gray, G. S.; Mosher, R.; Kallakury, B. V. Correlation of primary tumor prostate-specific membrane antigen expression with disease recurrence in PCa. *Clinical Cancer Research An Official Journal of the American Association for Cancer Research* **2003,** *9*, (17), 6357-6362.

13. Ali, A. O.; Zechmann, C. M.; Anna, M.; Matthias, E.; Michael, E.; Linhart, H. G.; Tim, H. L.; Hadaschik, B. A.; Giesel, F. L.; Jürgen, D. Comparison of PET imaging with a68Ga-labelled PSMA ligand and18F-choline-based PET/CT for the diagnosis of recurrent PCa. *European Journal of Nuclear Medicine & Molecular Imaging* **2014,** *41*, (1), 11-20.

14. Trover, J. K.; Beckett, M. L.; Jr, G. L. W. Detection and characterization of the prostate‐specific membrane antigen (PSMA) in tissue extracts and body fluids. *International Journal of Cancer* **1995,** *62*, (5), 552-558.

15. Ghosh, A.; Heston, W. D. Tumor target prostate specific membrane antigen (PSMA) and its regulation in PCa. *Journal of Cellular Biochemistry* **2004,** *91*, (3), 528.

16. Qhattal, H. S.; Liu, X. Characterization of CD44-mediated cancer cell uptake and intracellular distribution of hyaluronan-grafted liposomes. *Molecular pharmaceutics* **2011,** *8*, (4), 1233-46.

17. Liu, T.; Wu, L. Y.; Kazak, M.; Berkman, C. E. Cell-Surface labeling and internalization by a fluorescent inhibitor of prostate-specific membrane antigen. *Prostate* **2008,** *68*, (9), 955–964.

18. Nanus, D. M.; Milowsky, M. I.; Kostakoglu, L.; Smith-Jones, P. M.; Vallabahajosula, S.; Goldsmith, S. J.; Bander, N. H. Clinical use of monoclonal antibody HuJ591 therapy: targeting prostate specific membrane antigen. *Journal of Urology* **2003,** *170*, (2), 89-100.

19. Kozikowski, A. P.; Nan, F.; Conti, P.; Zhang, J.; Ramadan, E.; Bzdega, T.; Wroblewska, B.; Neale, J. H.; Pshenichkin, S.; Wroblewski, J. T. Design of remarkably simple, yet potent urea-based inhibitors of glutamate carboxypeptidase II (NAALADase). *Journal of medicinal chemistry* **2001,** *44*, (3), 298.

20. Peng, Z. H.; Sima, M.; Salama, M. E.; Kopeckova, P.; Kopecek, J. Spacer length impacts the efficacy of targeted docetaxel conjugates in prostate-specific membrane antigen expressing PCa. *Journal of drug targeting* **2013,** *21*, (10), 968-980.

21. Roy, J.; Nguyen, T. X.; Kanduluru, A. K.; Venkatesh, C.; Lv, W.; Reddy, P. V.; Low, P. S.; Cushman, M. DUPA conjugation of a cytotoxic indenoisoquinoline topoisomerase I inhibitor for selective PCa cell targeting. *Journal of medicinal chemistry* **2015,** *58*, (7), 3094-3103.

22. Liu, H.; Rajasekaran, A. K.; Moy, P.; Xia, Y.; Kim, S.; Navarro, V.; Rahmati, R.; Bander, N. H. Constitutive and antibody-induced internalization of prostate-specific membrane antigen. *Cancer research* **1998,** *58*, (18), 2674-2681.

23. Kularatne, S. A.; Venkatesh, C.; Santhapuram, H. K.; Wang, K.; Vaitilingam, B.; Henne, W. A.; Low, P. S. Synthesis and biological analysis of prostate-specific membrane antigen-targeted anticancer prodrugs. *Journal of medicinal chemistry* **2010,** *53*, (21), 7767-7777.

24. Luo, C.; Sun, J.; Sun, B.; Liu, D.; Miao, L.; Goodwin, T. J.; Huang, L.; He, Z. Facile Fabrication of Tumor Redox-Sensitive Nanoassemblies of Small-Molecule Oleate Prodrug as Potent Chemotherapeutic Nanomedicine. *Small* **2016,** *12*, (46), 6353-6362.

25. Kularatne, S. A.; Wang, K.; Santhapuram, H. K.; Low, P. S. Prostate-specific membrane antigen targeted imaging and therapy of PCa using a PSMA inhibitor as a homing ligand. *Molecular pharmaceutics* **2009,** *6*, (3), 780.

26. Akhtar, N. H.; Pail, O.; Saran, A.; Tyrell, L.; Tagawa, S. T. Prostate-specific membrane antigen-based therapeutics. *Advances in urology* **2012,** *2012*, 973820.

27. Elsässer-Beile, U.; Bühler, P.; Wolf, P. Targeted therapies for prostate cancer against the prostate specific membrane antigen. *Current Drug Targets* **2009,** *10*, (2),118 -125.

28. Lushchak, V. I. Glutathione homeostasis and functions: potential targets for medical interventions. *J Amino Acids* **2012,** *2012*, 736837.

29. Lee, F. Y.; Vessey, A.; Rofstad, E.; Siemann, D. W.; Sutherland, R. M. Heterogeneity of glutathione content in human ovarian cancer. *Cancer research* **1989,** *49*, (19), 5244.

30. Yin, Q.; Shen, J.; Zhang, Z.; Yu, H.; Li, Y. Reversal of multidrug resistance by stimuli-responsive drug delivery systems for therapy of tumor. *Advanced drug delivery reviews* **2013,** *65*, (13-14), 1699.

For Table of Contents Use Only

Prostate Specific Membrane Antigen Targeted Therapy of Prostate Cancer Using a DUPA–Paclitaxel Conjugate

Qingzhi Lv,[†‡] Jincheng Yang,[§] Ruoshi Zhang,[†] Zimeng Yang,[†] Zhengtao Yang,[§] Yongjun Wang,[†] Youjun Xu,*[§] Zhonggui He*[†]*

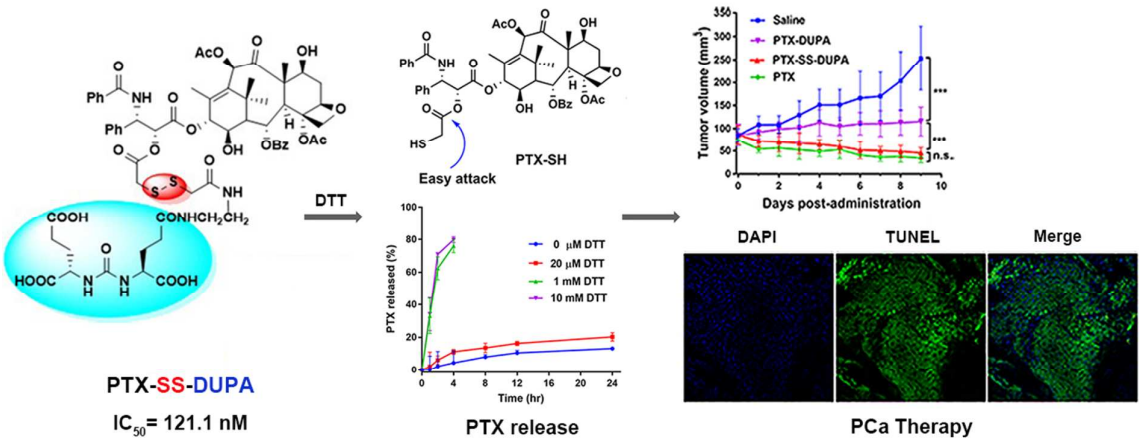

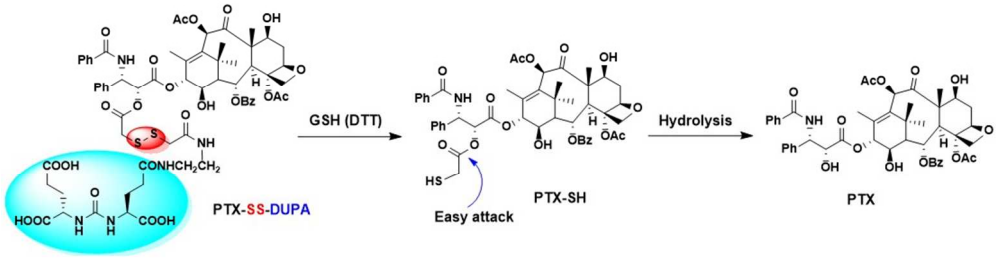

Scheme 1

294x77mm (96 x 96 DPI)

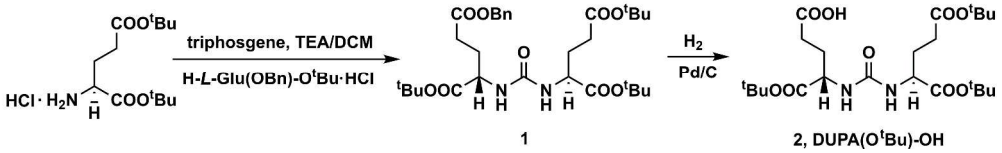

Scheme 2

1316x197mm (96 x 96 DPI)

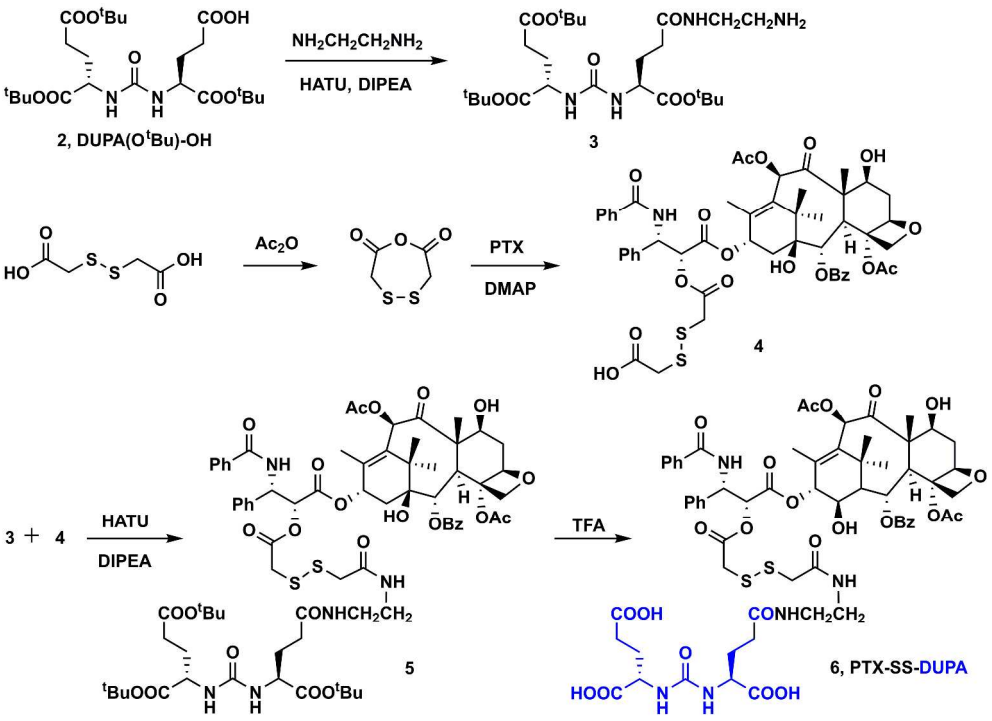

Scheme 3

1285x925mm (96 x 96 DPI)

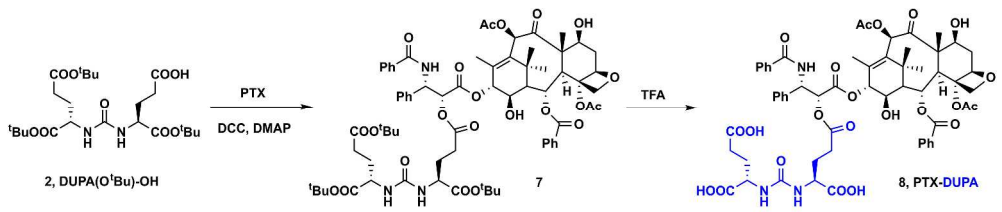

Scheme 4

1740x366mm (96 x 96 DPI)

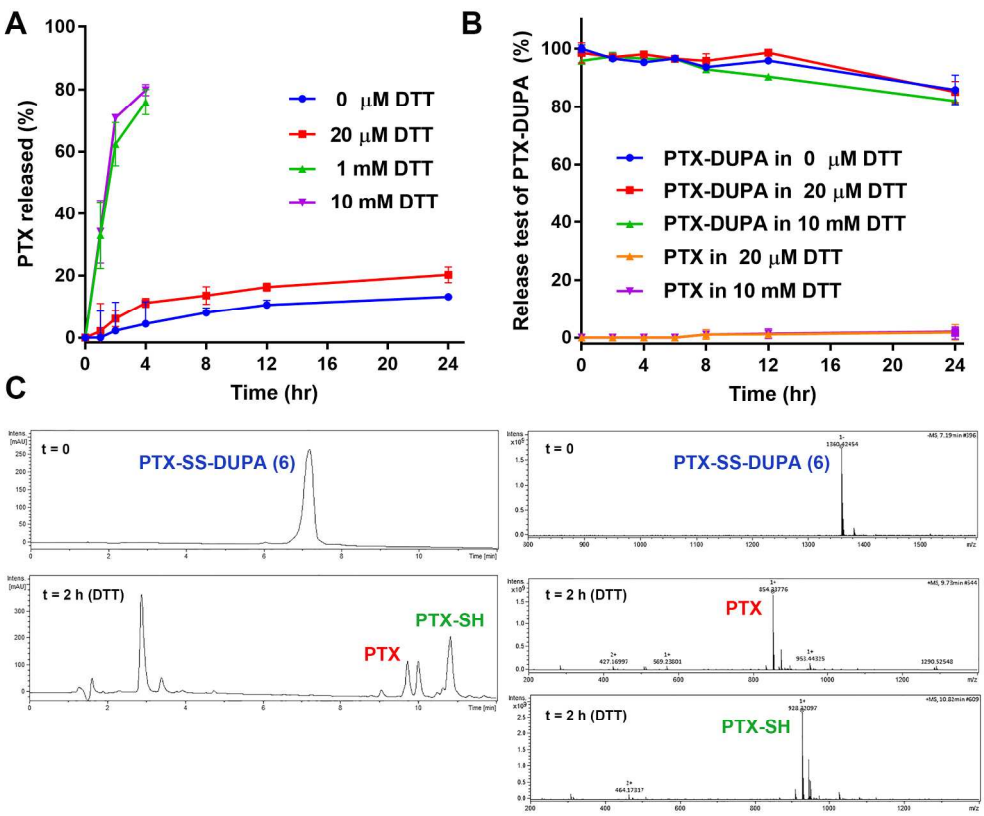

Figure 1

640x524mm (96 x 96 DPI)

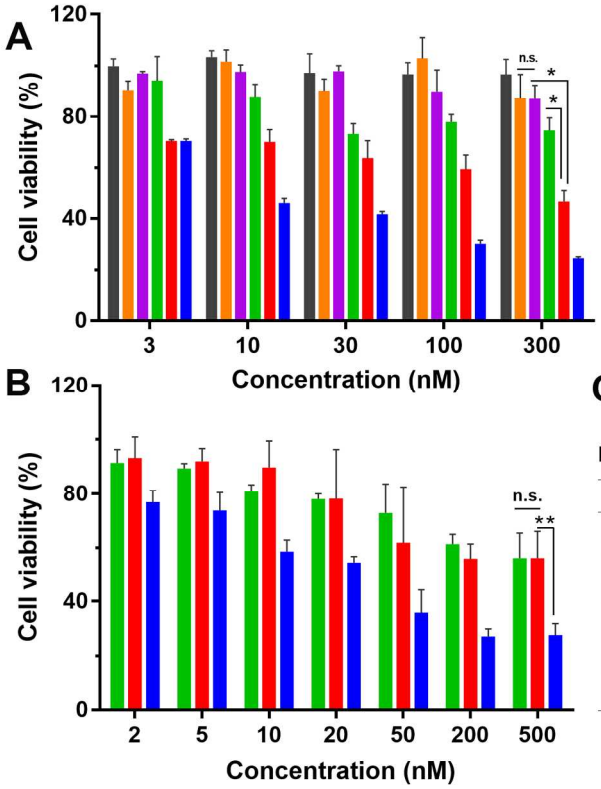

C

IC_{50} of PTX and DUPA-conjugates (nM)

	PC-3	22RV1
PTX	26.87	14.25
PTX-SS-DUPA	478.9	121.1
PTX-DUPA	822.4	563.3
PTX-SS-DUPA (P+)		1705
PTX-DUPA (P+)		2396
PMPA		431528

Figure 2

527x422mm (96 x 96 DPI)

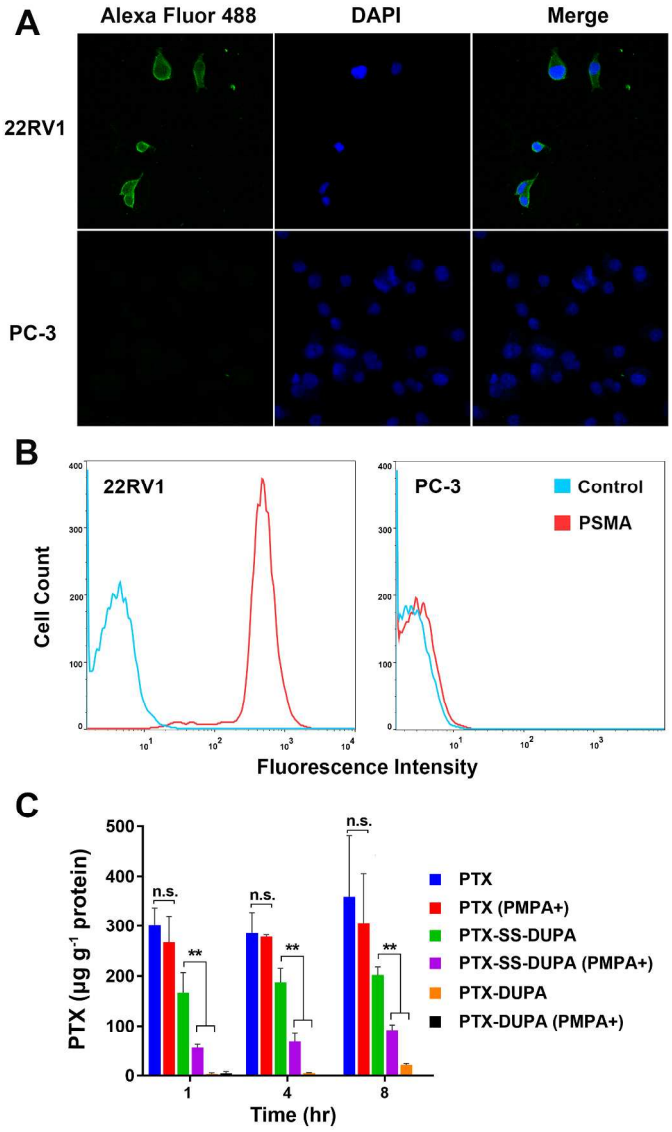

Figure 3

230x289mm (300 x 300 DPI)

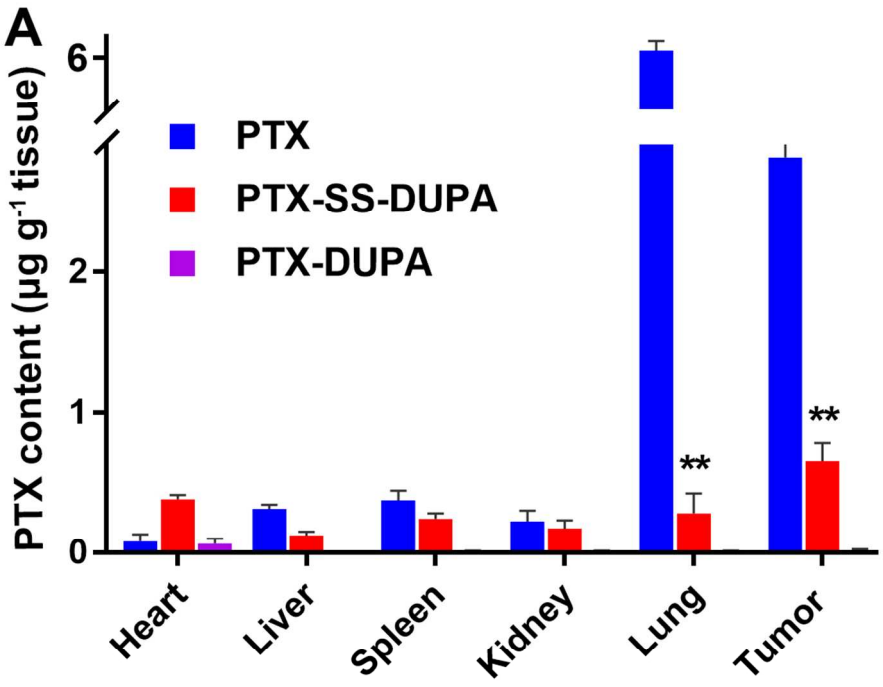

B PTX content in tissues (μg g^{-1} tissue)

Tissue \ Group	PTX	PTX-SS-DUPA	PTX-DUPA
Heart	0.08 ± 0.05	0.38 ± 0.03	0.06 ± 0.04
Liver	0.31 ± 0.03	0.12 ± 0.03	-
Spleen	0.37 ± 0.07	0.24 ± 0.04	-
Lung	6.35 ± 0.46	0.28 ± 0.14	-
Kidney	0.22 ± 0.08	0.17 ± 0.06	-
Tumor	2.81 ± 0.62	0.65 ± 0.13	0.01 ± 0.01

Figure 4

311x405mm (96 x 96 DPI)

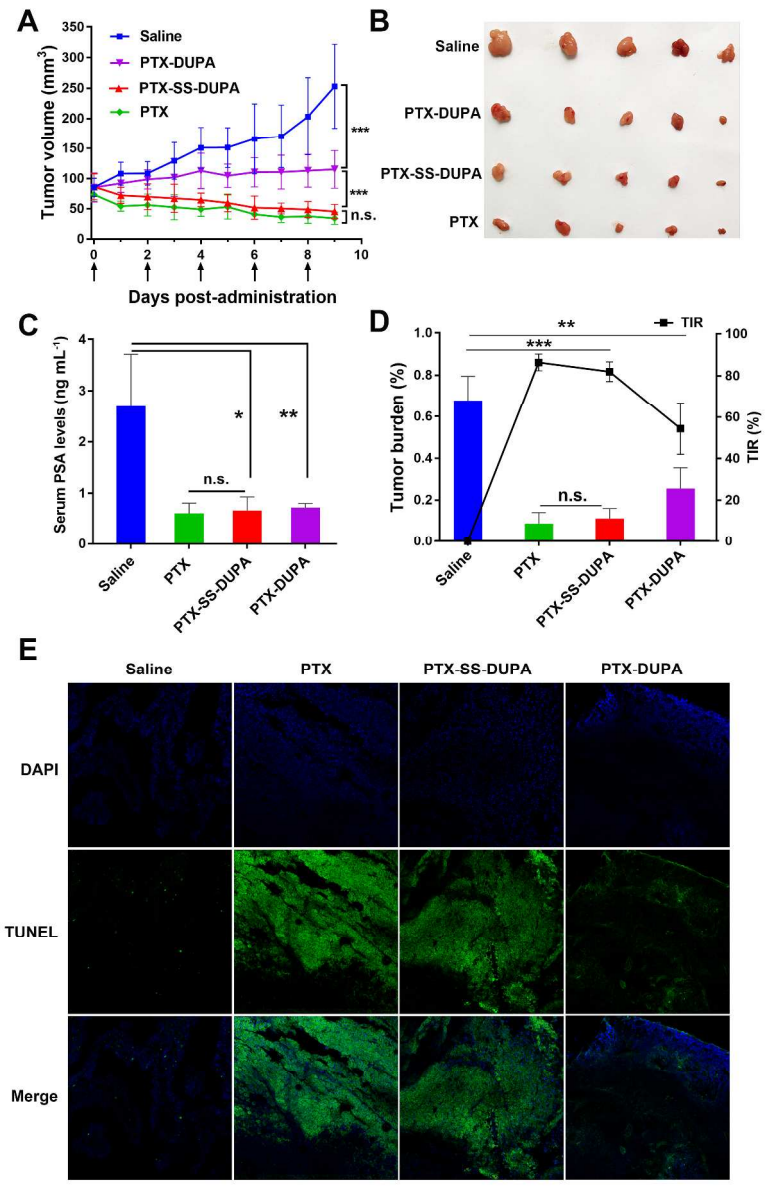

Figure 5

681x1058mm (96 x 96 DPI)

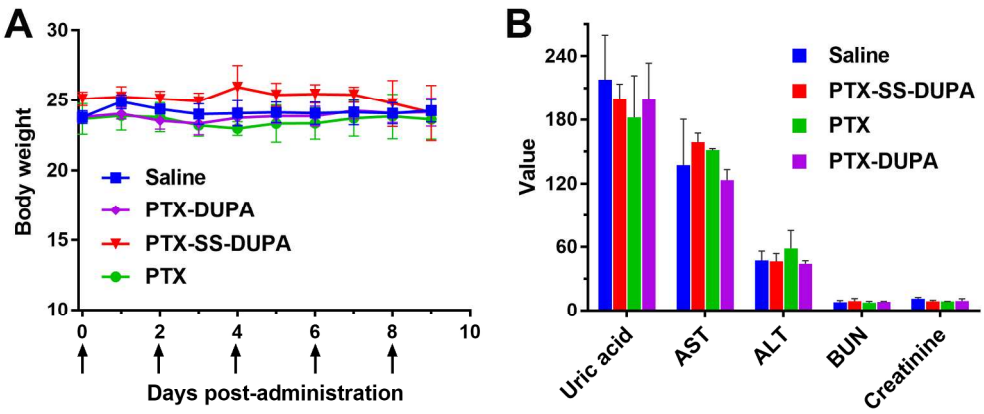

Figure 6

608x260mm (96 x 96 DPI)

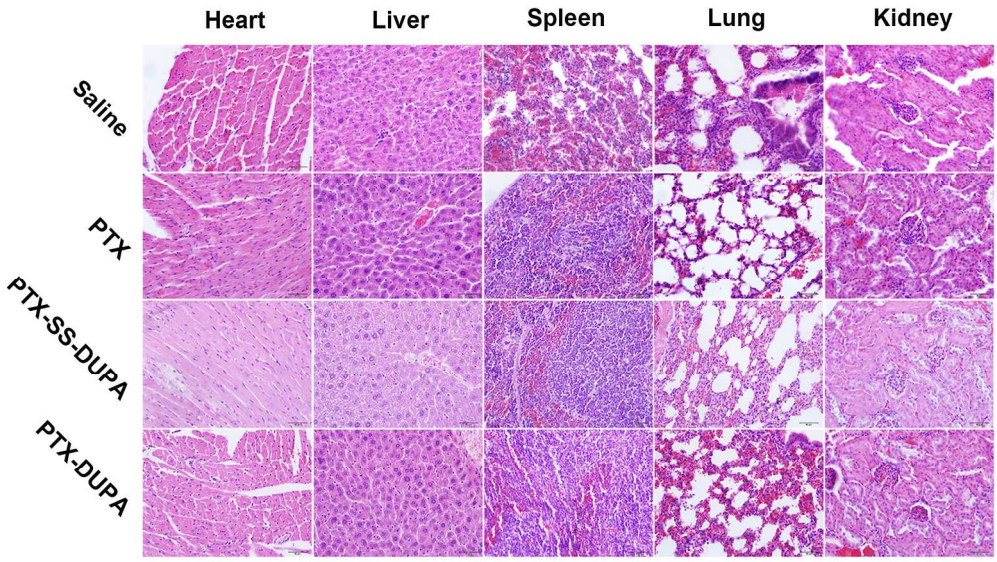

Figure 7

599x339mm (96 x 96 DPI)

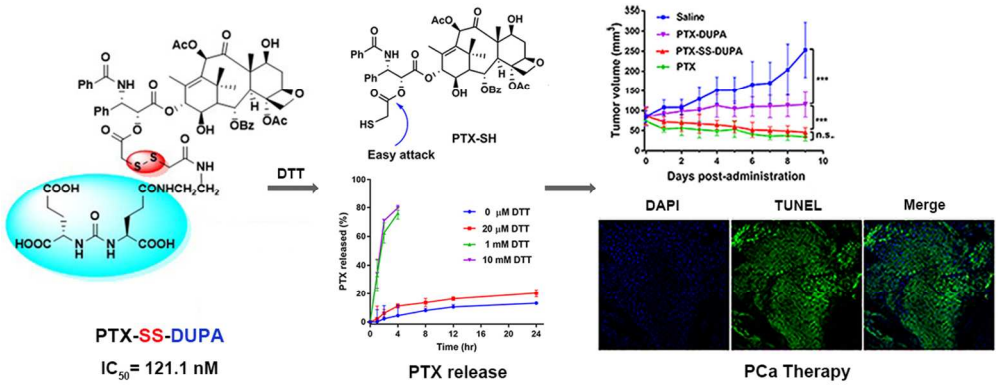

Table of Contents

444x179mm (72 x 72 DPI)